PROCEEDINGS, Thirty-Seventh Workshop on Geothermal Reservoir Engineering
Stanford University, Stanford, California, January 30 - February 1, 2012
SGP-TR-194

DOUBLE-DIFFERENCE ELASTIC-WAVEFORM INVERSION WITH WEIGHTED GRADIENTS FOR MONITORING EGS RESERVOIRS

Zhigang Zhang, Lianjie Huang, and Youzuo Lin

Los Alamos National Laboratory
Geophysics Group, Mail Stop D443
Los Alamos, New Mexico, 87545
E-mails: zzhang@lanl.gov, ljh@lanl.gov, ylin@lanl.gov

1. ABSTRACT

Reliably monitoring for enhanced geothermal systems (EGS) is crucial for placement of production wells and optimizing production of geothermal resources. We develop an improved double-difference elastic-waveform inversion method with weighted gradients for monitoring EGS reservoir changes utilizing time-lapse seismic data. We employ the gradients weighted by P- and S-wave energies in elastic-waveform inversion to improve reconstructed P- and S-velocity models using the baseline seismic data. Our new method well reconstructs the deep and shallow structures while the conventional waveform inversion produces poor reconstructions for the deep structures. We apply the weighted gradients to our double-difference elastic-waveform inversion method, and make use of a priori knowledge of the locations of EGS reservoirs to further improve quantification of geophysical property changes in EGS reservoirs. Our numerical example using a Brady's EGS model shows that our new double-difference elastic-waveform inversion method can quantitatively reconstruct time-lapse changes within EGS reservoirs. In addition, our new method significantly reduce image noise outside the EGS reservoir compared to those obtained using the conventional waveform inversion.

2. INTRODUCTION

In an EGS reservoir, cold water is injected into the hot basement rock through an injection well. Water is heated as it flows through the reservoir rock along induced fracture pathway. Monitoring the water pathways is necessary for managing and optimizing production of geothermal resources. Time-lapse seismic surveys could be an effective, non-invasive monitoring tool.

In the conventional waveform inversion of time-lapse seismic data, reservoir changes are obtained by subtracting the results of independently inversion of each time-lapse dataset. The resulting images are usually noisy. This is because the structures outside the reservoirs have to be inverted by both of the two independent inversions, and the difference of the image noises of the two independent inversions are still image noises.

Watanabe et al. (2004) used the differences in acoustic transmission data (cross-well seismic data) to invert for reservoir changes. Deli and Huang (2009) developed a double-difference waveform inversion method to improve inversion of time-lapse seismic reflection data. Double-difference elastic-waveform inversion method jointly inverts for changes in geophysical properties in EGS reservoirs using time-lapse seismic reflection data. The method consists of two steps: Inversion of the baseline data for the initial compressional- (P-) and shear-wave (S-wave) velocity models, and reconstruction of geophysical property changes within an EGS reservoir using differences of time-lapse seismic data. The image noise of double-difference elastic-waveform inversion is much fewer than that of conventional inversion of time-lapse seismic data.

Conventional elastic-waveform inversion of surface reflection seismic data usually reconstructs the shallow region of a model much better than the deep region, because seismic energy is stronger in the shallow region than that in the deep region. We balance the gradient during elastic-waveform inversion using seismic wave energy to significantly improve reconstructions of the deep region of the model (Zhang, et al., 2011).

In this paper, we use our elastic-waveform inversion method with weighted gradients and the baseline data to invert for the baseline P- and S-velocity models. We also apply the weighted gradients to our double-difference elastic-waveform inversion to enhance the fidelity of reconstructions. The approximate location

of the geothermal reservoir is known. We employ this spatial *a priori* information in the double-difference elastic-waveform inversion to further improve reconstructions of both the location and magnitude of the geophysical property changes. We use a numerical example to demonstrate that our new double-difference elastic waveform inversion with weighted gradients is a promising tool for quantitatively monitoring for EGS reservoirs.

3. METHODS

3.1. Elastic-waveform inversion

Elastic-waveform inversion in the time domain minimizes the misfit function given by

$$E = \sum_{(s,r)} \frac{1}{2} \int dt [\tilde{\mathbf{u}}(\mathbf{x}_r, \mathbf{x}_s) - \tilde{\mathbf{d}}(\mathbf{x}_r, \mathbf{x}_s)]^T \cdot [\tilde{\mathbf{u}}(\mathbf{x}_r, \mathbf{x}_s) - \tilde{\mathbf{d}}(\mathbf{x}_r, \mathbf{x}_s)], \quad (1)$$

where $\tilde{\mathbf{u}}$ is the synthetic wavefield at receiver r from source s, $\tilde{\mathbf{d}}$ is the data at receiver r from source s, and the superscript T represents the transpose.

In inversion, we update the model according to:

$$\mathbf{m}_{k+1} = \mathbf{m}_k + \alpha_k \boldsymbol{\gamma}_k, \quad (2)$$

where $\mathbf{m}$ is the model parameters, $\boldsymbol{\gamma}$ the gradient of the misfit function, α a step length, k an iteration number.

A commonly used method to minimize E is the adjoint gradient method (Tarantola, 1984; Pratt, 1999; Tromp, 2005). The gradient is given by

$$\boldsymbol{\gamma} = -\frac{\partial E}{\partial \mathbf{m}}, \quad (3)$$

and

$$\frac{\partial E}{\partial \mathbf{m}} = \sum_{(s)} \delta \mathbf{d}^T \frac{\partial \tilde{\mathbf{u}}}{\partial \mathbf{m}} (\mathbf{x}_r, \mathbf{x}_s), \quad (4)$$

where $\delta \mathbf{d} = \sum_{(r)} [\tilde{\mathbf{u}}(\mathbf{x}_r, \mathbf{x}_s) - \tilde{\mathbf{d}}(\mathbf{x}_r, \mathbf{x}_s)]$.

For elastic media, if we assume constant density, the wavefield perturbation is given by

$$\delta \tilde{\mathbf{u}} = -2\rho\alpha \int_V \delta\alpha dV \int_\tau [\nabla \cdot G(\mathbf{x}, t-\tau; \mathbf{x}_r) \nabla \cdot u(\mathbf{x}, \tau; \mathbf{x}_s)] d\tau - 4\rho\beta \int_V \delta\beta dV \int_\tau \grave{o}^G_{nj}(\mathbf{x}, t-\tau; \mathbf{x}_r) \grave{o}^u_{nj}(\mathbf{x}, \tau; \mathbf{x}_s) d\tau \quad (5)$$

where G is the Green's function, $\grave{o}$ the strain tensor; α the P-wavespeed, β the S-wavespeed. The perturbation of misfit function is then written as

$$\delta E = -\sum_{(s)} \{2\rho\alpha \int_V \delta\alpha dV \int_t [\nabla \cdot b(\mathbf{x}, t; \mathbf{x}_r) \nabla \cdot u(\mathbf{x}, t; \mathbf{x}_s)] dt + 4\rho\beta \int_V \delta\beta dV \int_t b_{n,j}(\mathbf{x}, t; \mathbf{x}_r) \grave{o}^u_{nj}(\mathbf{x}, t; \mathbf{x}_s) dt\}. \quad (6)$$

The P-wavespeed gradient is

$$\gamma_\alpha = \sum_{(s)} 2\rho\alpha \int_V \delta\alpha dV \cdot \int_t [\nabla \cdot b(\mathbf{x}, t; \mathbf{x}_r)][\nabla \cdot u(\mathbf{x}, t; \mathbf{x}_s)] dt. \quad (7)$$

The S-wavespeed gradient is

$$\gamma_\beta = \sum_{(s)} 2\rho\beta \int_V \delta\beta dV \cdot \int_t [b_{n,j}(\mathbf{x}, t; \mathbf{x}_r) \grave{o}^u_{nj}(\mathbf{x}, t; \mathbf{x}_s)] dt. \quad (8)$$

3.2. Elastic-waveform inversion with elastic-wave energy-weighted gradients

To compensate the wave propagation effect, Choi et al (2008) defined a new pseudo-Hessian with the diagonal term:

$$diag\{(\mathbf{H})_{new-p}\} = \sum \mathbf{Re}\{(\mathbf{f}_{s,1})^T \mathbf{A} (\mathbf{f}_{s,1})^* \ldots (\mathbf{f}_{s,M})^T \mathbf{A} (\mathbf{f}_{s,M})^*\}, \quad (9)$$

with

$$diag\{\mathbf{A}\} = \mathbf{Re}\{\sum_{s=1}^{n_s} |g_{s,1}| \ldots \sum_{s=1}^{n_s} |g_{s,2n}|\}, \quad (10)$$

where g is the impulse response, n_s is the number of sources, and n is the number of model grid points. However, this compensates for only the wave propagation effect from sources, not from receivers.

We scale the gradient with an elastic-wave energy gradient method (Zhang, et al., 2010). If we define two weight factors as

$$W_s \equiv \sum_s u^2, \quad (11)$$

and

$$W_r \equiv \sum_s b^2, \quad (12)$$

where *u* is the forward propagated wavefield from a source and *b* is the back propagated wavefield from a receiver . The elastic-wave energy weighted gradient is given by

$$\gamma_w = \frac{\gamma}{(W_s W_r)^{1/2}}. \quad (13)$$

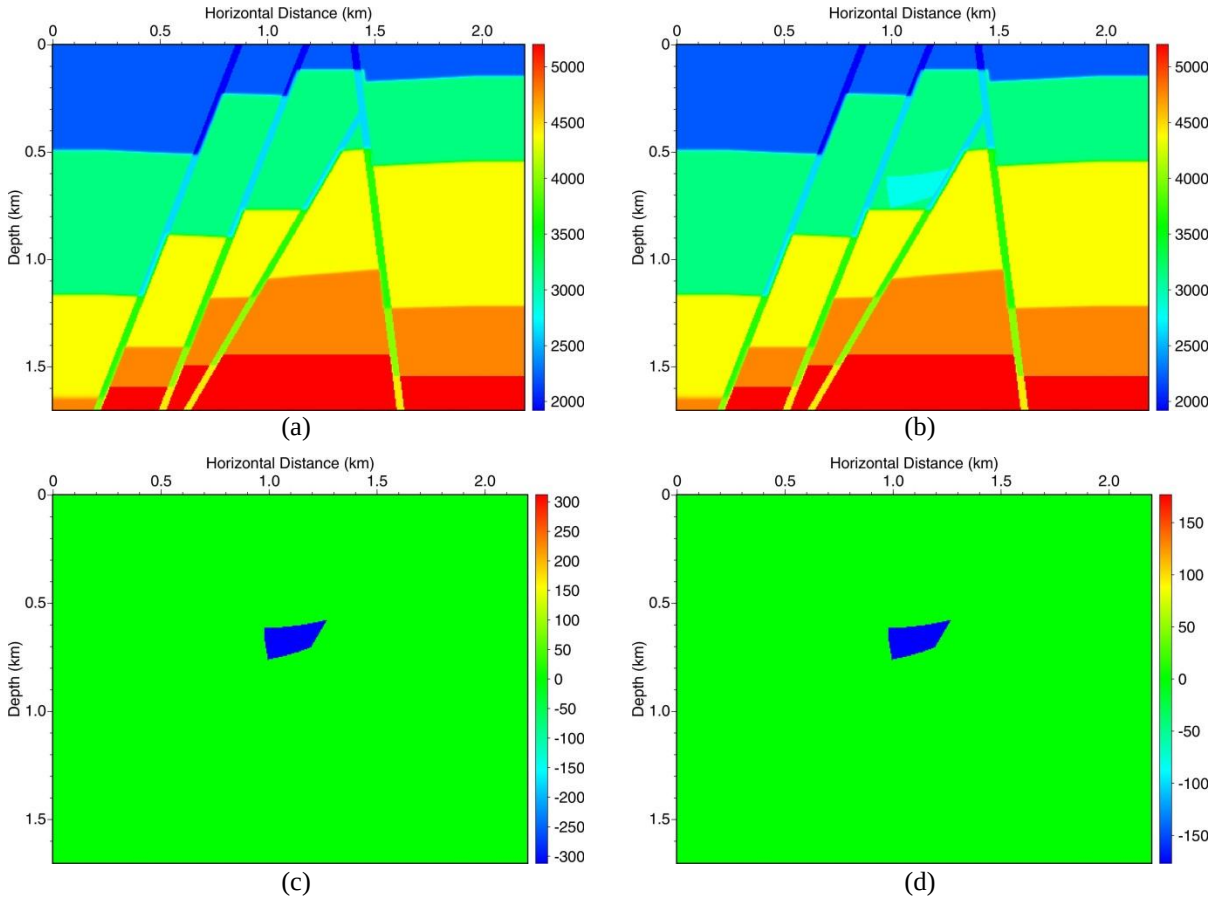

Figure 1. The time-lapse P-wave velocity models (a and b). The time-lapse S-wave velocity models have the same pattern, but only different in magnitude. (c) and (d) are the P- and S- wave velocity differences between the time-lapse models.

3.3. Double-difference elastic-waveform inversion

Using the elastic-wave energy weighted gradient in eq. (13), the waveform inversion of the baseline data leads to model $\tilde{\mathbf{m}}_0$. We make the simulated time-lapse data as

$$u_{sim} = u(\tilde{\mathbf{m}}_0) + (d_1 - d_0), \tag{14}$$

where $u(\tilde{\mathbf{m}}_0)$ is the simulated data from the model $\tilde{\mathbf{m}}_0$, and d_1 and d_0 are time-lapse seismic data acquired at two different times. To perform waveform inversion using data u_{sim}, we obtain a time-lapse model $\tilde{\mathbf{m}}_1$. The data misfit used for double-difference elastic-waveform inversion is given by

$$\delta d = [u(\tilde{\mathbf{m}}_1) - u(\tilde{\mathbf{m}}_0)] - (d_1 - d_0), \tag{15}$$

where $u(\tilde{\mathbf{m}}_1)$ is the simulated data for the reconstructed time-lapse model $\tilde{\mathbf{m}}_1$. The time-lapse geophysical property change is

$$\Delta\mathbf{m} = \tilde{\mathbf{m}}_1 - \tilde{\mathbf{m}}_0. \tag{16}$$

When δd vanishes, which implies that the inversion converges, we have

$$u(\tilde{\mathbf{m}}_1) - u(\tilde{\mathbf{m}}_0) = d_1 - d_0. \tag{17}$$

The difference of the simulated time-lapse data equals to the difference of the true time-lapse data.

Since the data difference is caused by the time-lapse changes of the geophysical properties within the reservoir, eq. (17) means that the result of eq. (16) is essentially the true difference of the time-lapse velocity models, even though $\tilde{\mathbf{m}}_0$ and $\tilde{\mathbf{m}}_1$ may not be the true baseline and time-lapse models. Although double-difference elastic-waveform inversion does require a good baseline model, it has a much higher tolerance of the inaccuracy in baseline model than the conventional waveform inversion method, because only the difference of the time-lapse data matters in the double-difference elastic-waveform inversion.

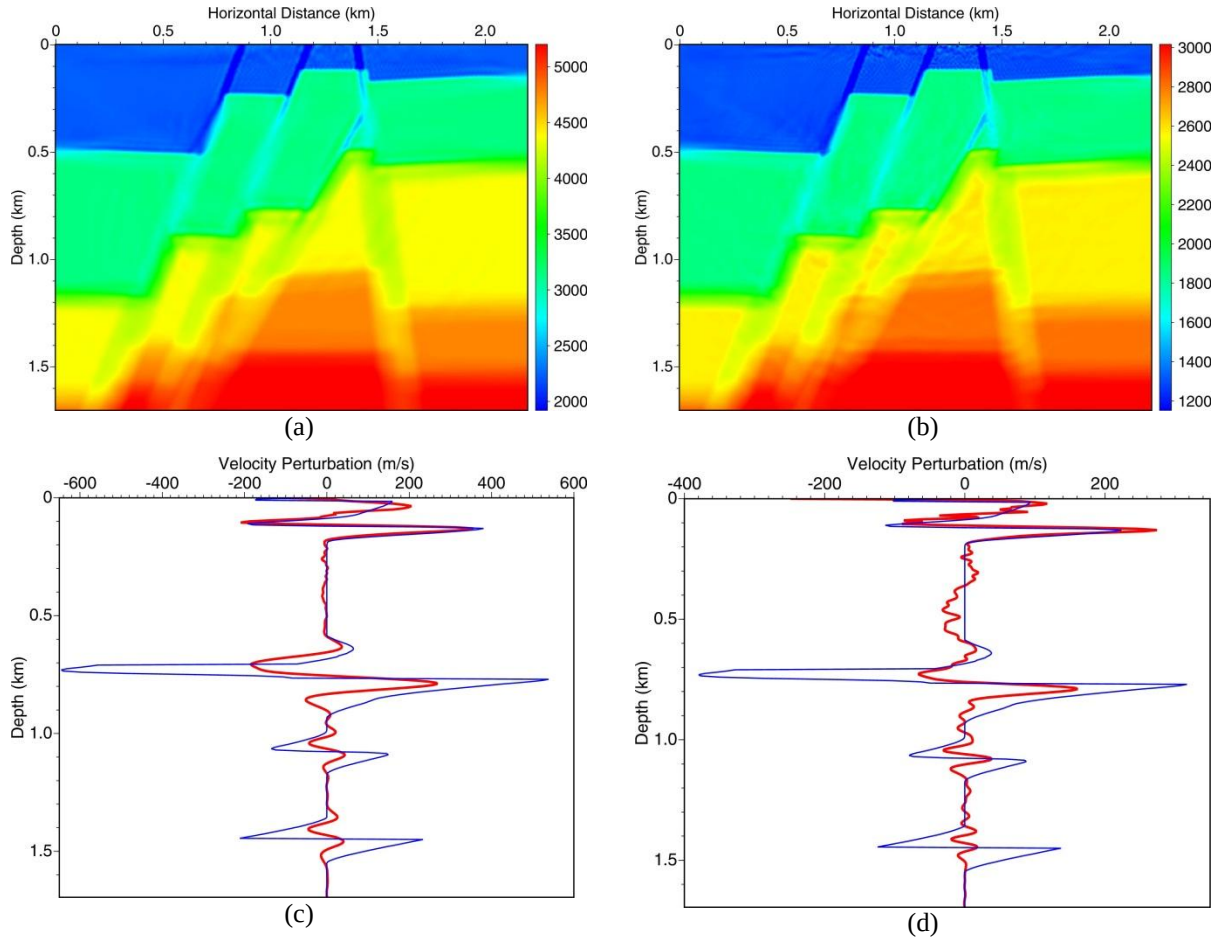

Figure 2. P- (a) and S- (b) velocities reconstructed using the conventional elastic-waveform inversion method. Only the shallow region is well reconstructed, but the deep part is smeared. Two vertical profiles (c) and (d) are at the horizontal location of 1.1 km in (a) and (b) subtracted by the initial models, respectively. The horizontal axis of (c) and (d) is the velocity change, and the vertical axis is the depth. The blue lines are the true magnitude, and the red lines are the inversion result.

4. NUMERICAL EXAMPLE

We use a Brady's EGS model to test our double-difference elastic-waveform inversion method with weighted gradients. The model consists of several steep faults (Fig. 1). The geothermal reservoir is assumed to be at depths from 550 m to 800 m. We generate synthetic seismic reflection data for 100 sources and 450 receivers located on the top surface of the model. The central frequency of the source wavelet is 25 Hz.

We first invert the P- and S-velocity structure of the baseline model using elastic-waveform inversion. When applying elastic-waveform inversion to surface seismic reflection data, one difficulty is that the deep region of the model is usually not reconstructed as well as the shallow region (Fig. 2). It has been recognized that this phenomenon is caused by the uneven spatial distribution of seismic energy in the model. The shallow region is well reconstructed, but the deep region is blurred (Figs 2a and b). The two vertical profiles in Figs. 2c and d show comparisons of true velocity models and reconstructed results minus the initial model at the horizontal location of 1.1 km. The blue lines are the difference between the true models and the initial models, and the red lines are the difference between the reconstruction results and the initial models (Figs. 2c and d).

Our new elastic-wave energy-weighted method uses elastic-wave energies of forward and backward propagated wavefields from sources and receivers as weights to compute the gradients during elastic-waveform inversion. The result in Fig. 3 shows that all the features in the model are well reconstructed, including the steep faults in the deep region.

We simulate synthetic data using the reconstructed baseline model, and then generate the simulated time-

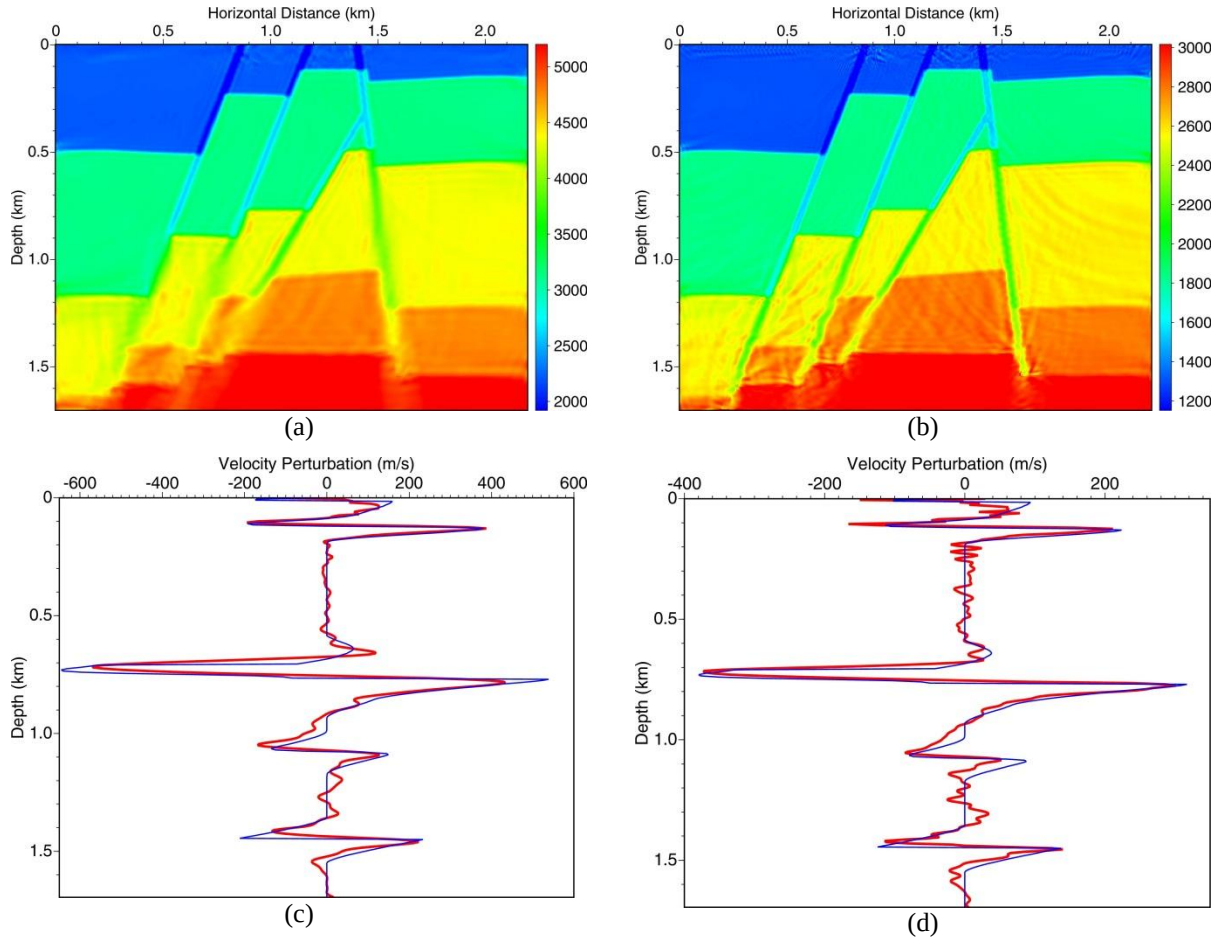

Figure 3. P- (a) and S- (b) velocities reconstructed using elastic-waveform inversion with elastic-wave energy-weighted gradients. Almost all the features are well reconstructed for both P- and S- velocities. Two vertical profiles (c) and (d) are at the horizontal location of 1.1 km in (a) and (b) subtracted by the initial models, respectively. The horizontal axis of (c) and (d) is the velocity change, and the vertical axis is the depth. The blue lines are the true magnitude, and the red lines are the inversion results.

lapse data by summing up the synthetic data and the difference of the true time-lapse data. Using the reconstructed baseline model as an initial model and the simulated time-lapse data, we conduct the elastic-waveform inversion again. In this inversion, the update of model parameters focuses on the changes within the EGS reservoir because inconsistency between the data and model is only the difference of the time-lapse data. The result is shown in Fig. 4. The location and shape of the velocity change within the EGS reservoir has been well reconstructed (Figs. 4a and b). The vertical profiles at the horizontal location of 1.1 km show that the magnitude of time-lapse velocity changes has been fully reconstructed for both P- and S- velocities (Figs. 4c and d).

5. CONCLUSIONS

Our elastic-waveform inversion with elastic-wave energy-weighted gradients significantly improves reconstructions of the deep region of the model, particularly the structures around the EGS reservoir and steep faults, which help quantify reservoir changes. Our double-difference elastic-waveform inversion with elastic-wave energy-weighted gradients focuses image reconstruction using the difference in time-lapse seismic data. The method enables the application of spatial *a priori* information to enhance reconstructions and reduce image artifacts. Our numerical example demonstrates that both the location and magnitude of changes of geophysical properties within an EGS reservoir are well reconstructed using our double-difference full-waveform inversion with elastic-wave energy-weighted gradients and spatial *a priori* information of the EGS reservoir.

6. ACKNOWLEDGEMENTS

This work was supported by the Geothermal Technologies Program of the U.S. Department of Energy through contract DE-AC52-06NA25396 to

Los Alamos National Laboratory. We thank Dr. John Queen of Hi-Q Geophysical Inc. for providing us with a velocity model of the Brady's EGS field.

REFERENCES

Choi, Y., Min, D. J. and Shin, E. (2008), "Frequency-domain full-waveform inversion using the new pseudo-Hessian matrix: Experience of elastic Marmousi-2 synthetic data" *Bull. seism. Soc. Am.*, **98**, 2402-2415.

Denli, H., and Huang, L. (2009), "Double-Difference Elastic Waveform Tomography in the Time Domain" *SEG Technical Program Expanded Abstracts*, 2302-2306.

Pratt, R. G., Shin, C. and Hicks, G. J. (1998), "Gauss-Newton and full Newton methods in frequency-space seismic waveform inversion" *Geophysical Journal International*, **133**, 341-362.

Tromp, J. Tape, C. and Liu, Q. (2005), "Seismic tomography, adjoint methods, time reversal and banana-doughnut kernels" *Geohphysical Journal International*, **160**, 195-216.

Watanabe, T., Shimizu, S., Asakawa, E. and Matsuoka, T. (2004), "Differential waveform tomography for time-lapse crosswell seismic data with application to gas hydrate production monitoring" *SEG Technical Program Expanded Abstracts*, 2302-2306.

Zhang, Z., Lin, Y. and Huang, L. (2011), "Full-waveform inversion in the time domain with an energy-weighted gradient" *SEG Technical Program Expanded Abstracts*, 2772-2776.

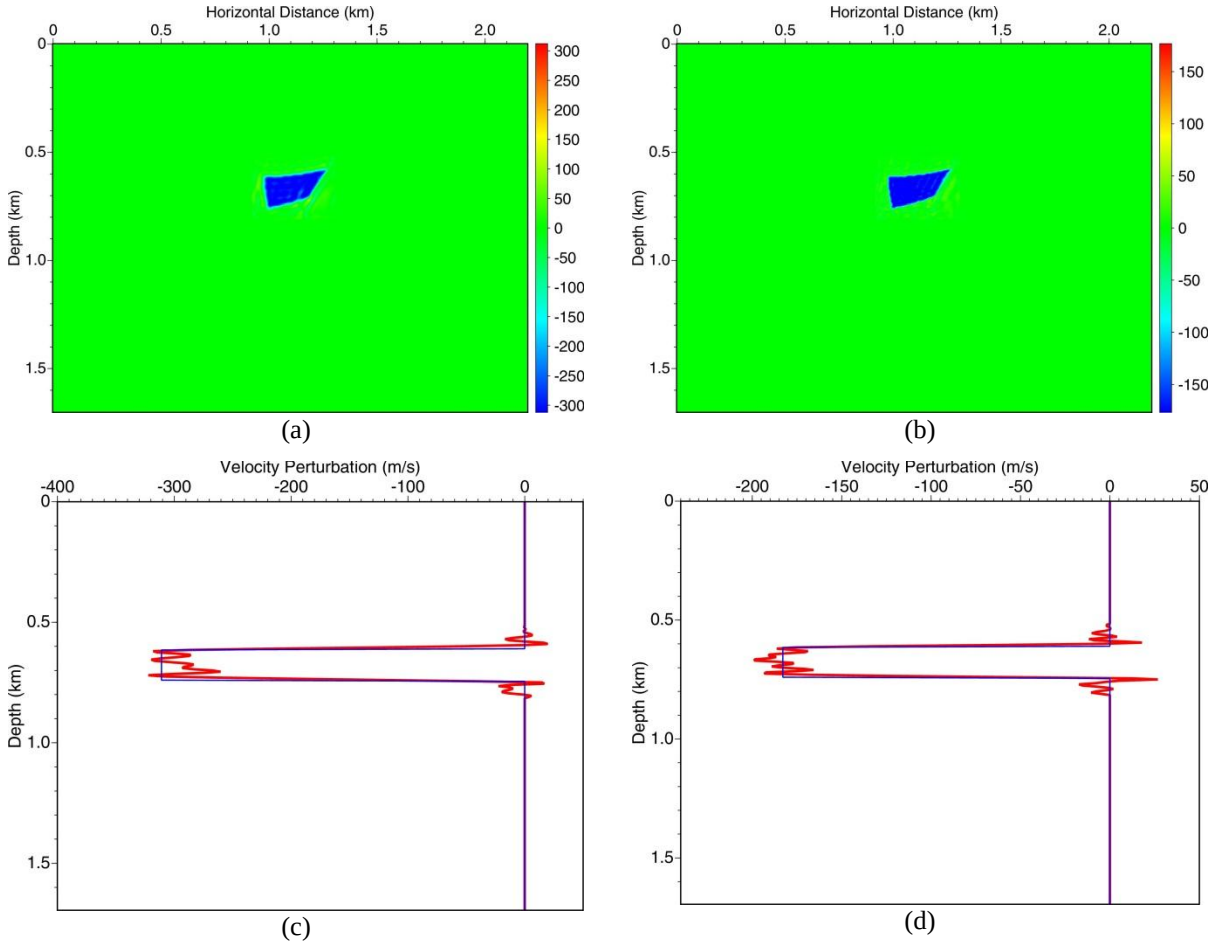

Figure 4. The time-lapse change of P- (a) and S- (b) velocities reconstructed using double-difference elastic elastic-waveform inversion with elastic-wave energy-weighted gradients and the spatial a priori information of the EGS reservoir. Two vertical profiles (c) and (d) are at the horizontal location of 1.1 km in (a) and (b). The horizontal axis of (c) and (d) is the magnitude of the velocity change, and the vertical axis is the depth. The blue lines are the true magnitude, and the red lines are the results of (a) and (b). Both the location and the magnitude of the time-lapse changes are well reconstructed.